# Supporting Information :
# Interfacial interactions as an electrochemical tool to understand Mo-based catalysts for the hydrogen evolution reaction

Nicolas Dubouis,[1] Chunzhen Yang,[1], Robin Beer,[1] Lucie Ries,[2] Damien Voiry[2] and Alexis Grimaud*[1,3,4]

[1]Collège de France, 11 Place Marcelin Berthelot, 75231 Paris, France
[2]IEM, University of Montpellier, CNRS, ENSCM, Montpellier 34095, France
[3]Réseau sur le Stockage Electrochimique de l'Energie (RS2E), FR CNRS 3459, France
[4]Sorbonne Universités - UPMC Univ. Paris 06, 4 place Jussieu, F-75005 Paris, France

*Alexis Grimaud alexis.grimaud@college-de-france.fr

# Supporting Information

## Calculations for model proposed in Fig. 4

## Detailed calculations for the model

This model was inspired by two models proposed elsewhere in the literature : one proposed by Takanabe K. *et al.* by considering the different HER mechanisms but ignoring diffusion effects[1] and a second one proposed by Markovic *et al.* considering only one mechanism but using Levich equation to simulate an RDE experiment[2].

### Assumptions considered

1. Three main assumptions were considered :
   (a) Volmer step $H_3O^+ + e^- + M \underset{k_{-v}}{\overset{k_v}{\rightleftharpoons}} H_{ads} + H_2O$, $K_V$
   (b) Heyrovsky step $H_{ads} + H_3O^+ + e^- \underset{k_{-h}}{\overset{k_h}{\rightleftharpoons}} H_2 + M + H_2O$, $K_H$
   (c) Tafel step $2H_{ads} \underset{k_{-t}}{\overset{k_t}{\rightleftharpoons}} H_2 + 2\,M$, $K_T$
2. As Argon (Ar) was bubbled through the solution and thanks to the rotation of the electrode it was assumed $[H_2]_{bulk}=[H_2]_{interface}=0$. This approximation is probably not accurate because at high current densitites, bubbles on the working electrode could be noticed.
3. Same approximation was done for $O_2$ : $[O_2]_{bulk}=[O_2]_{interface}=0$.
4. Three limit cases were studied 1) Volmer rate limiting step 2) Volmer Heyrovsky, Heyrovsky rate limiting step , 3) Volmer Tafel, Tafel rate limiting step
5. Mass transport was assumed governed by the diffusion of the species, the rotation speed of our electrode and the current. Thus, concentration of a chemical species A at the interface of the electrode was assumed to be given by the following expression :

$$[A]_{x=0}=[A]_{bulk} + \frac{j}{2Fm_A} \tag{1}$$

   where $m_A$ is given by the Levich equation :

$$m_A = 0.620\omega^{1/2}\nu^{-1/6}D_A^{2/3} \tag{2}$$

   where $\omega$ is the rotation speed of the electrode, $\nu$ the kinematic viscosity of the solution and $D_A$ the diffusion coefficient of the species A in the solution.
6. Butler-Volmer equation was used to express current densities, with a pre-exponential rate constant $k_i$ including a kinetic factor, the spectators ions influence, and other effects not

explicited in this study.

$$k_i = k_i^\circ \exp\left[-\alpha_i f(E - E^\circ_{H^+/H_2})\right] \tag{3a}$$

$$k_{-i} = k_{-i}^\circ \exp\left[(1-\alpha_{-i}) f(E - E^\circ_{H^+/H_2}))\right] \tag{3b}$$

$$f = F/RT \text{ and } \alpha \text{ the transfer coefficients} \tag{3c}$$

7. Finally, the current density $j$ was correlated with the reaction rate of the limiting step $r$ according to the following equation :

$$j = -nFr \tag{4}$$

**Modeling**

**Volmer limiting step** The Volmer limiting step is the simpliest case. As the adsorption step is limiting, the coverage $\theta$ can be assumed to be close to 0. Then the reaction rate can be derived as shown bellow :

$$[\mathrm{H_3O^+}][(1-\theta)] \simeq [\mathrm{H_3O^+}] \tag{5a}$$

$$r = r_v = [\mathrm{H_3O^+}][(1-\theta)] \simeq [\mathrm{H_3O^+}]k_v = [\mathrm{H_3O^+}]k_v^\circ \exp(-\alpha_v f(E - E^\circ_{H^+/H_2})) \tag{5b}$$

$$j = -2F[\mathrm{H_3O^+}]k_v^\circ \exp(-\alpha_v f(E - E^\circ_{H^+/H_2})) \tag{5c}$$

$$\text{with } [\mathrm{H_3O^+}] = [\mathrm{H_3O^+}]_{\text{bulk}} + \frac{j}{2Fm_{\mathrm{H_3O^+}}} \tag{5d}$$

**Heyrovsky limiting step** With Heyrovsky step as the rate limiting step, we should assume the Volmer step to be in a quick equilibrium so we have :

$$k_v[\mathrm{H_3O^+}](1-\theta) = k_{-v}\theta[\mathrm{H_2O}] \tag{6a}$$

$$\theta = \frac{K_V^\circ[\mathrm{H_3O^+}]}{[\mathrm{H_2O}]\exp(f(E - E^\circ_{H^+/H_2})) + K_V^\circ[\mathrm{H_3O^+}]} \tag{6b}$$

then we have for the rate limiting step :

$$r = r_h = k_h\theta[\mathrm{H_3O^+}] \tag{7a}$$

$$j = -nF\frac{k_h^\circ K_V^\circ[\mathrm{H_3O^+}]^2 \exp\left(-\alpha_h f(E - E^\circ_{H^+/H_2})\right)}{[\mathrm{H_2O}]\exp(f(E - E^\circ_{H^+/H_2})) + K_V^\circ[\mathrm{H_3O^+}]} \tag{7b}$$

$$\text{with } [\mathrm{H_3O^+}] = [\mathrm{H_3O^+}]_{\text{bulk}} + \frac{j}{2Fm_{\mathrm{H_3O^+}}} \tag{7c}$$

**Tafel limiting step** As for Heyrovsky, Volmer was assumed to be in a quick equilibrium and same expression of the coverage was considered. As there are no electron transfers in the Tafel step, the kinetic constant can be assumed independant of the potential and current density is expressed as detailed by following equations :

$$k_t = k_t^\circ \tag{8a}$$

$$r = r_t = k_t \theta^2 \tag{8b}$$

$$j = -nFk_t^\circ \left[ \frac{K_V^\circ [\mathrm{H_3O^+}]}{[\mathrm{H_2O}] \exp(f(E - E^\circ_{H^+/H_2})) + K_V^\circ [\mathrm{H_3O^+}]} \right]^2 \tag{8c}$$

$$\text{with } [\mathrm{H_3O^+}] = [\mathrm{H_3O^+}]_{\text{bulk}} + \frac{j}{2Fm_{\mathrm{H_3O^+}}} \tag{8d}$$

**Computation and numerical assumptions**

To compute this model, Python scripts were used, using the Numpy package to solve non-linear equations. Only one solution to each equation was considered (a guess value was iteratively calculated)

Here are listed the values considered for the physical constants used in this study :

$n = 2$ (number of electrons exchanged)
$D_{H^+} = 8\ 10^{-9} \mathrm{m^2\ s^{-1}}$ (diffusion coefficient for proton in water[2])
$F = 96,500\ \mathrm{C\ mol^{-1}}$ (Faraday constant)
$R = 8.31\ \mathrm{J\ mol^{-1}\ K^{-1}}$(perfect gas constant)
$T = 298\ \mathrm{K}$
$K = 1\ \mathrm{e^{-8}}$
$k_v = 1\ \mathrm{e^{-8}\ s^{-1}}$
$k_h = 1\ \mathrm{e^{-4}\ m^3\ mol^{-1} s^{-1}}$
$k_t = 1\ \mathrm{e^{-8}\ m^3\ mol^{-1} s^{-1}}$
$\omega = 1,600$ rpm(electrode rotation speed)
$\nu = 8.9\ \mathrm{e^{-7}\ m^2\ s^{-1}}$
$\alpha = 0.5$

## S1: Tafel plot for bulk materials normalized with BET surface area

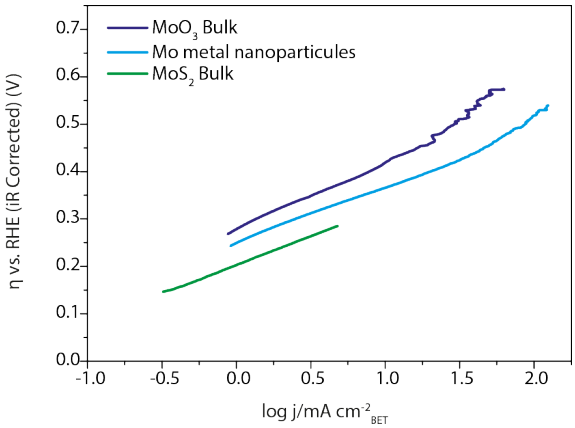


**Figure S1.** Tafel plot measured for an RDE experiment at pH 0 for bulk $MoO_3$ (dark blue), $Mo_{(M)}$ (light blue) and $MoS_2$ (green) normalized using BET surface area.

## S2: Dissolution of bulk $MoO_3$ and Mo particles during cycling at pH 0

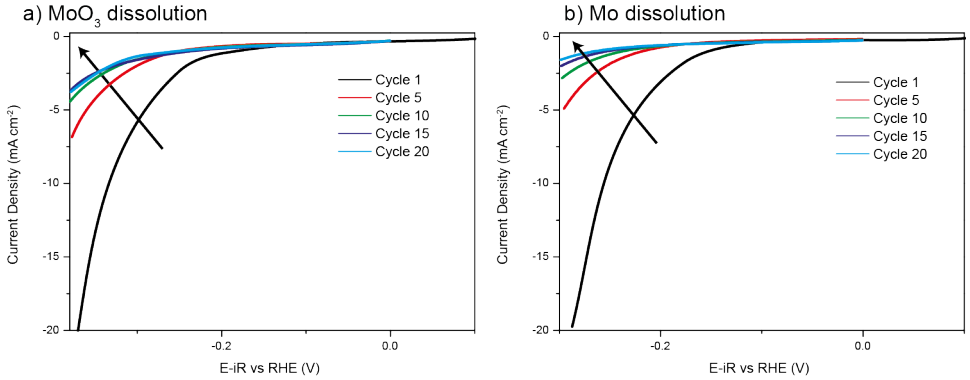


**Figure S2.** Polarization curves recorded in pH 0 electrolytes using RDE experiments at 1,600 rpm and 20 mV $s^{-1}$ on a) $MoO_3$ and b) $Mo_{(M)}$ electrodes showing dissolution of those bulk materials when cycled in strong acidic conditions. Electrodes tested here were previously activated by cycling them 20 times in a pH 4 electrolyte (as shown in Fig. S3).

## S3: Activation of bulk $MoO_3$ and Mo particles during cycling at pH 4

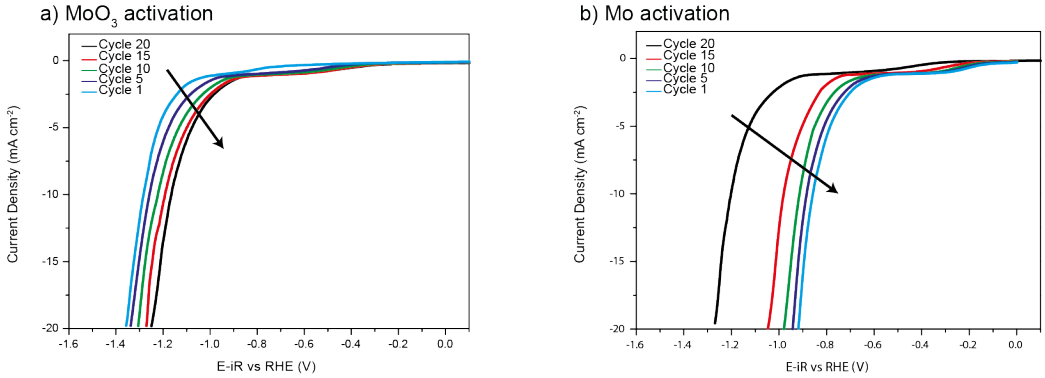


**Figure S3.** Polarization curves recorded in pH 4 electrolytes using RDE experiments at 1,600 rpm and 20 mV $s^{-1}$ on a) $MoO_3$ and b) $Mo_{(M)}$ electrodes revealing activation of these materials upon cycling.

## S4: pH dependence for Mo-based catalysts, comparison with Pt

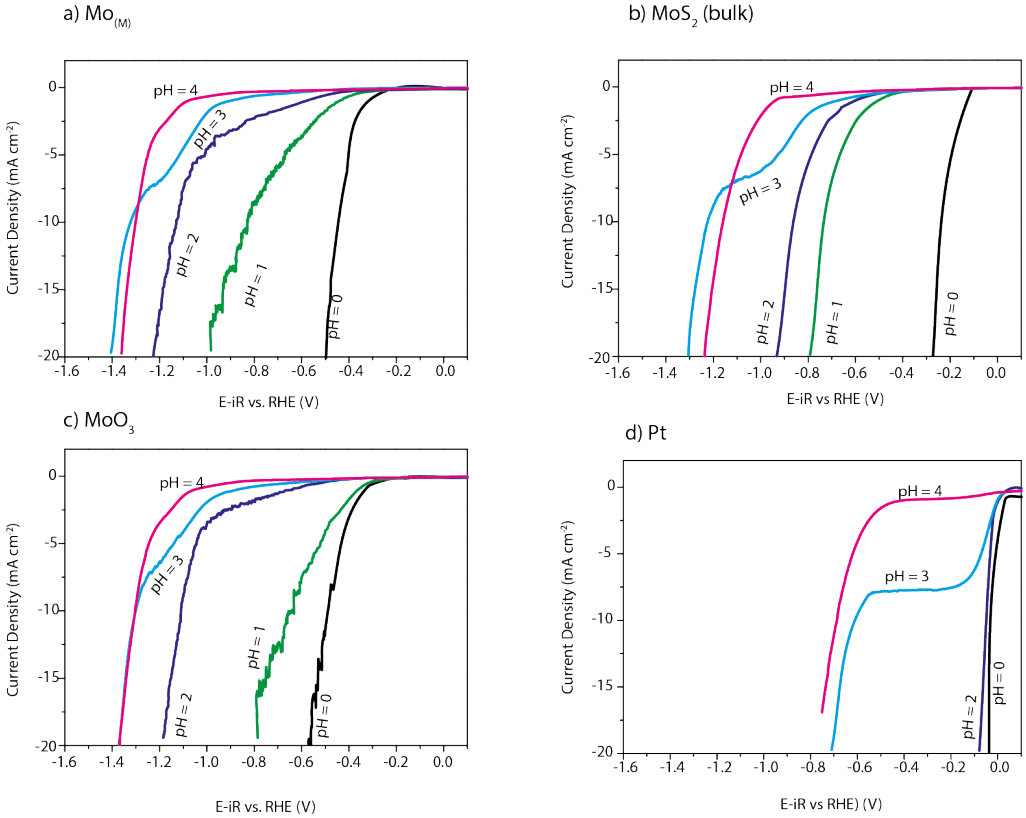


**Figure S4.** Polarization curves recorded in different pH conditions, using RDE experiments at 1,600 rpm and 20 mV $s^{-1}$ on several electrode materials showing the existence of two reduction mechanisms (proton and water) for all these materials.

## S5: pH dependence of the Tafel slopes for Pt electrode

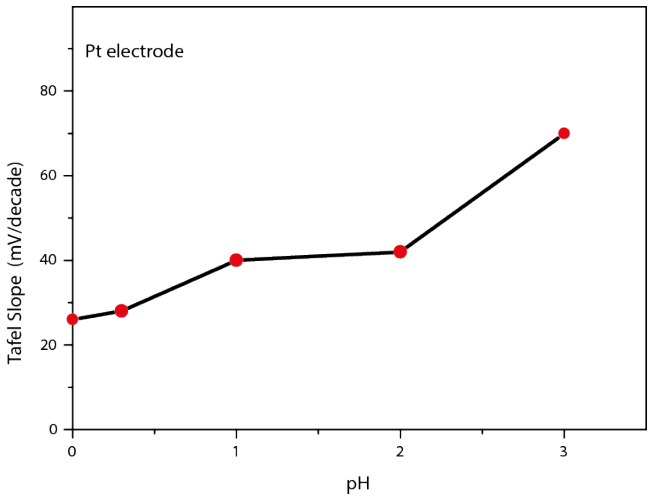


**Figure S5.** Evolution of the Tafel slope for a Pt planar electrode measured in different pH $H_2SO_4$ electrolytes using RDE setup (1,600 rpm, 20 mV $s^{-1}$). Plain line serves as a guide.

## S6: RDE performed at pH 3 on a-$MoS_x$ and 1T-$MoS_2$ using different cations

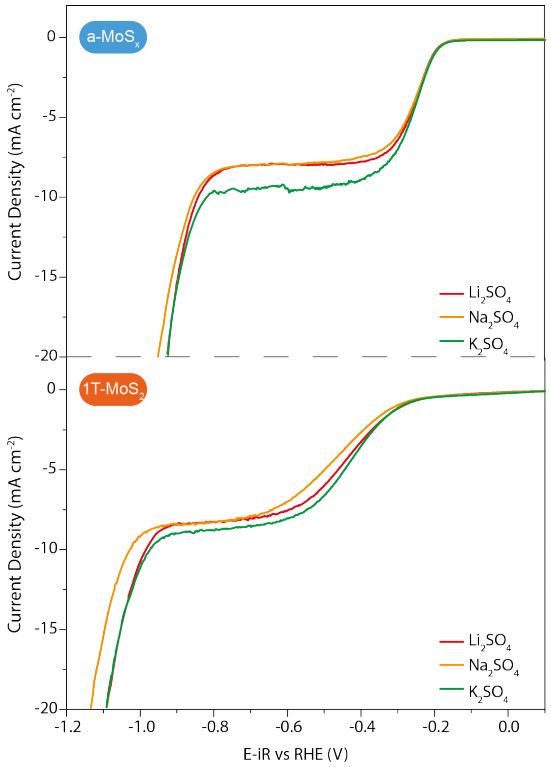


**Figure S6.** Polarization curves recorded in different pH 3 electrolytes using RDE experiments at 1,600 rpm and 20 mV $s^{-1}$ on a-$MoS_x$ (top) and exfoliated 1T-$MoS_2$ electrodes (bottom) showing no significant effect of the supporting electrolyte on the HER mechanism.

## S7: Cation influence on Pt electrode at pH 3

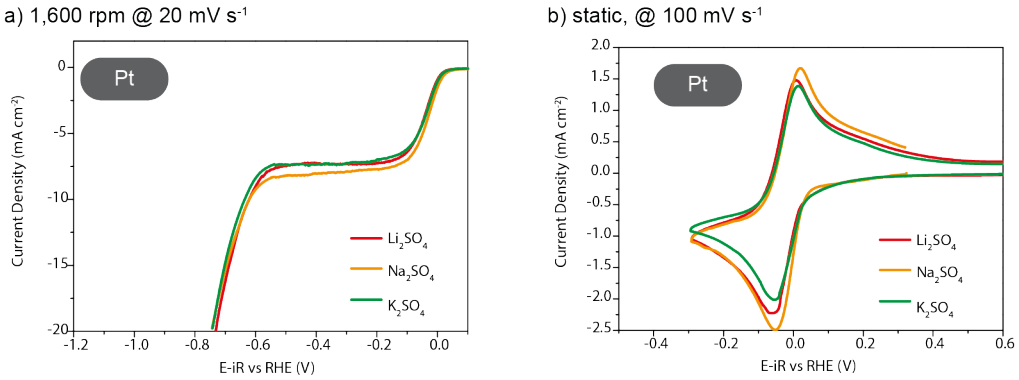


**Figure S7.** a) Polarization curves recorded in different pH 3 electrolytes using RDE experiments at 1,600 rpm and 20 mV $s^{-1}$ on a Pt electrode and b) static CV recorded at 100 mV $s^{-1}$ on a Pt electrode, both showing no significant effect of the supporting electrolyte on the HER mechanisms.

## S8: $H_2O/D_2O$ effect for Pt

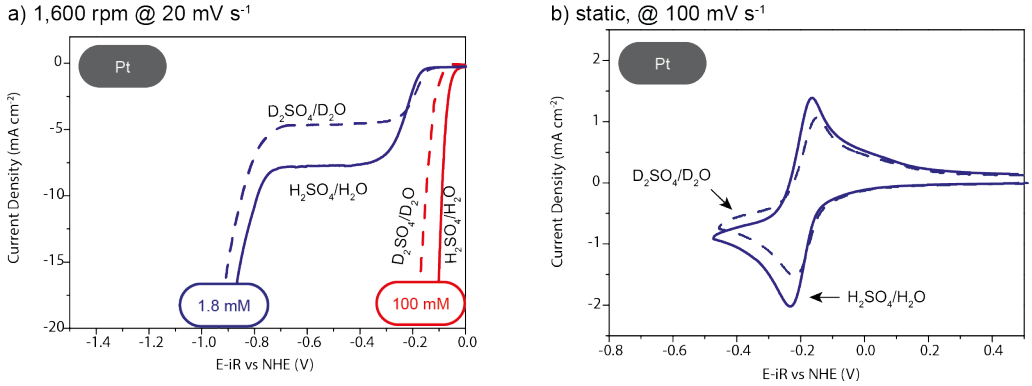


**Figure S8.** a) Polarization curves recorded in normal (plain lines) or deuterated electrolytes (dashed lines) 100 mM acid (red) and 1.8 mM (blue) at 20 mV $s^{-1}$ using a RDE at 1,600 rpm and b) corresponding static cyclovoltamograms recorded in the 1.8 mM acid electrolytes at 100 mV $s^{-1}$ over a Pt electrode showing the low influence of the isotopic effect on kinetics for the HER/DER.

## S9: Electrodeposition of a-$MoS_x$

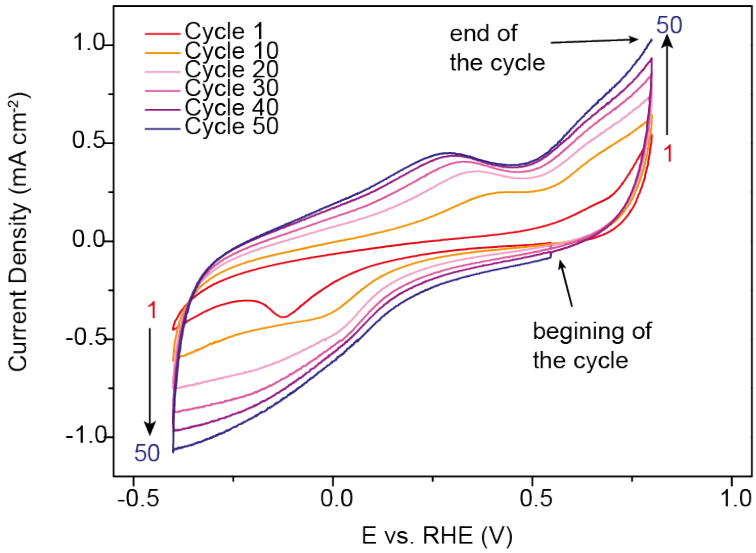


**Figure S9.** Electrodeposition of a-$MoS_x$ films on glassy carbon electrodes by performing 50 consecutive CV at 50 mV $s^{-1}$ in 1 mM $(NH_4)_2MoS_4$ electrolyte.

### 1T-$MoS_2$ preparation and characterization

### Physical characterization

X-Ray photoelectron spectroscopy (XPS) experiments were performed using a Thermo Scientific K-Alpha spectrometer. All spectra were taken using Al Kα micro focused monochromatized source (1486.7 eV) with a pass energy of 15 eV. The spot size for XPS analyses is 400 µm. Raman spectroscopy was carried out using an InVia Raman microscope (Renishaw) at excitation laser wavelength of 2.41 eV (514 nm).

### Synthesis of chemically exfoliated 1T $MoS_2$ nanosheets:

Exfoliated nanosheets of 1T $MoS_2$ were prepared *via* lithium intercalation following previous reports from the literature[3]. Briefly, under inert atmosphere, 0.3 g of bulk $MoS_2$ (Sigma-Aldrich) was mixed with 3 mL of n-butyllithium (Sigma-Aldrich, 1.6 M in hexane). The mixture was heated at reflux for 48 hours to allow intercalation of the $MoS_2$ crystals. The reaction was then stopped and Li-intercalated $MoS_2$ ($Li_xMoS_2$) powder was washed with hexane (Sigma-Aldrich, 4x50 mL) and dried. $Li_xMoS_2$ was then exfoliated in water at a concentration of 1 mg/mL with the aid of sonication. The solution was then washed via centrifugation in order to completely remove the lithium cations and the non-exfoliated $MoS_2$ aggregates[4].

## S10. Raman characterization of 1T $MoS_2$

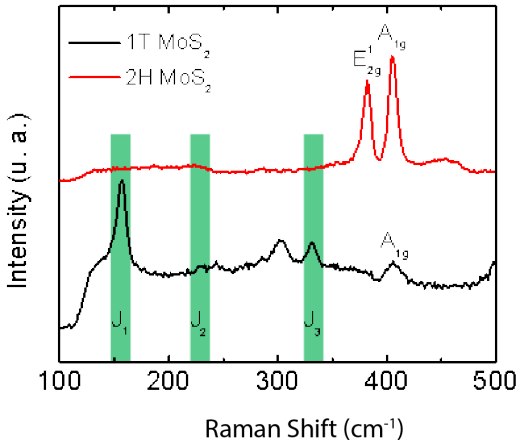


**Figure S10.** Raman spectra of chemically exfoliated 1T and 2H $MoS_2$ obtained at $\lambda_{exc}$=2.41 eV.

**Raman spectroscopy of 1T $MoS_2$**

Exfoliated $MoS_2$ nanosheets were characterized using micro-Raman spectroscopy at a laser excitation of 2.41 eV. 2H $MoS_2$ shows 2 main Raman modes $A_{1G}$ and $E^1_{2G}$ at 405.7 $cm^{-1}$ and 382.2 $cm^{-1}$. The conversion of 2H to the 1T phase induces the rise of novel Raman signals called $J_1$, $J_2$ and $J_3$ at 156.9; 229.2 and 331.7 $cm^{-1}$ respectively that are attributed to strained 1T phase of $MoS_2$ (Figure S10)[5].

## S11: X-Ray Photoelectron Spectroscopy (XPS) spectra of 1T $MoS_2$

Figure S11 shows the XPS spectra of the Mo3d and S2p regions of 1T and 2H $MoS_2$. The 1T phase of $MoS_2$ is known to be slightly downshifted relative to the 2H phase1. By fitting the raw XPS spectra, we can deconvolute the XPS signals into signals from the 2H and 1T phases. According to the deconvolution from the Mo3d and S2p, the amount of the 1T phase in the chemically exfoliated nanosheets (1T $MoS_2$) is estimated to be ~70%.

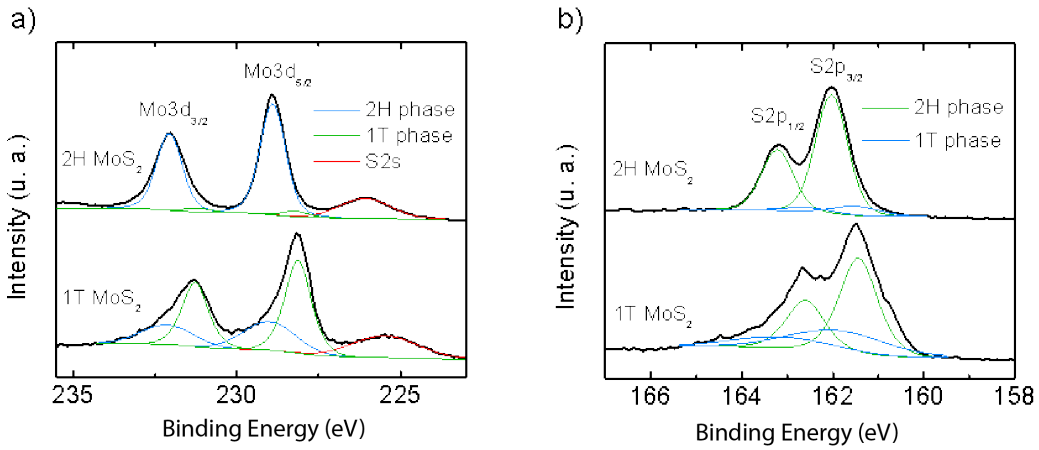


**Figure S11.** XPS spectra of chemically exfoliated 1T and 2H $MoS_2$.

## S12: Activation of a-$MoS_x$ at pH 0

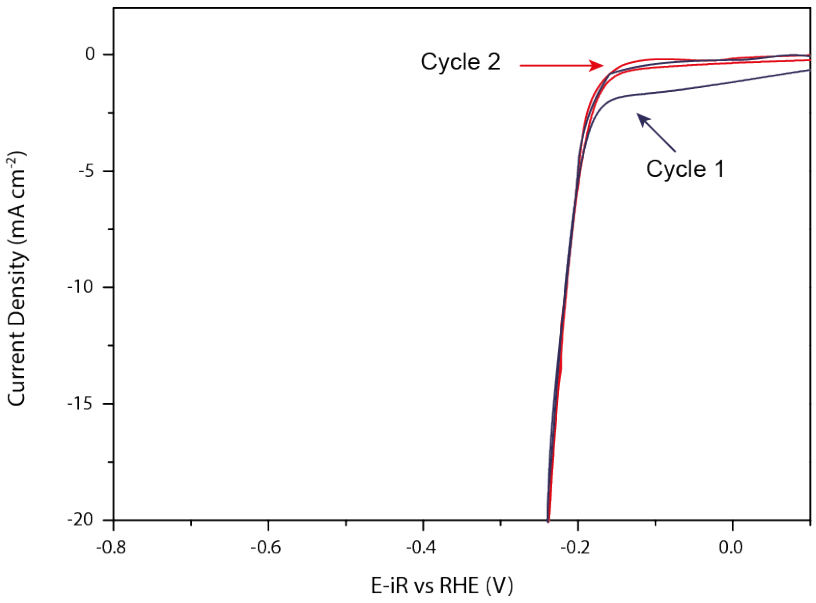


**Figure S12.** Activation of the a-$MoS_x$ electrode during the first cycle in 1M $H_2SO_4$ using RDE at 1,600 rpm and scanning at 20 mV $s^{-1}$.

## S13: Comparison of Pt and Graphite Rod as counter electrodes

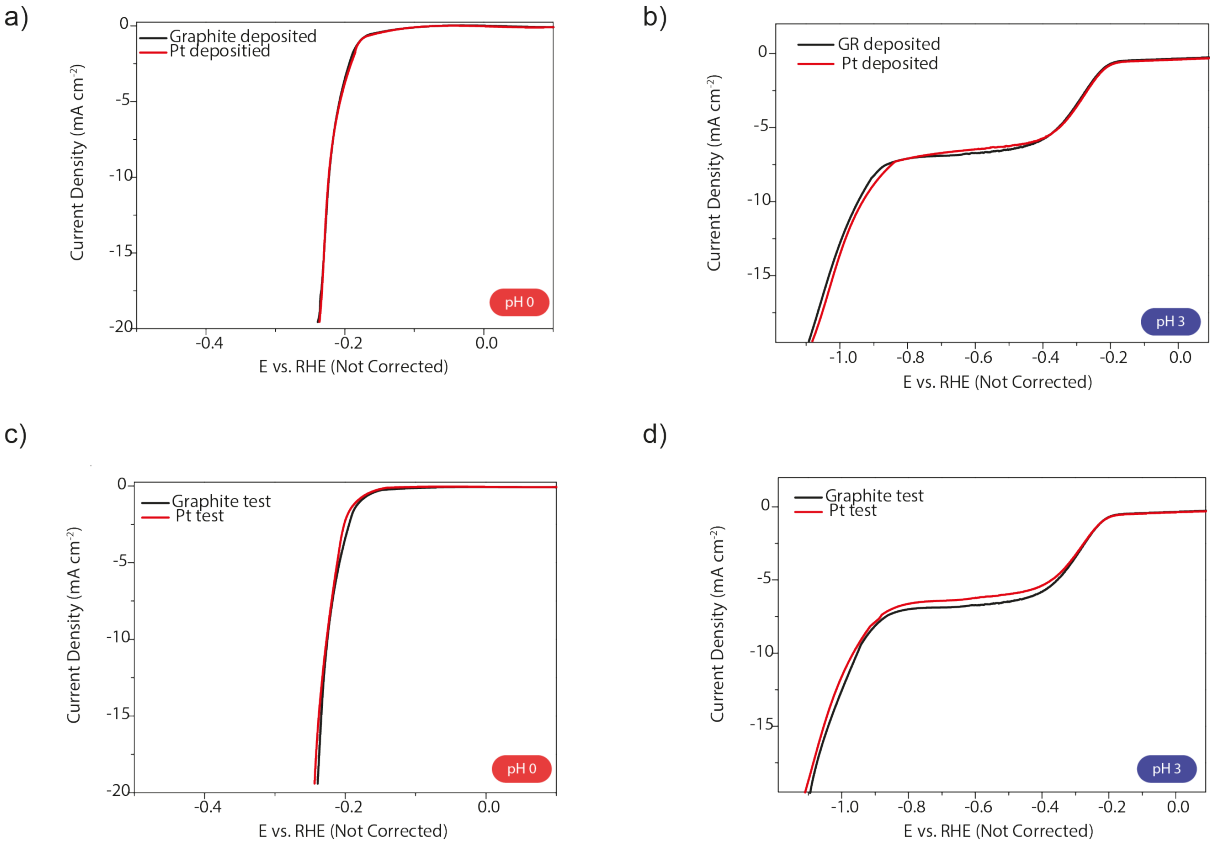


**Figure S13**. Amorphous $MoS_x$ electrodes deposited using either Pt (red) or graphite rod (black) counter electrodes were tested in a) pH 0 and b) pH 3 electrolytes using a graphite rod as counter electrode to confirm the absence of contamination during the deposition. Amorphous $MoS_x$ electrodes deposited using graphite were tested in c) pH 0 and d) pH 3 electrolytes using either a graphite rod (black) or a Pt wire (red) as counter electrodes to demonstrate the absence of contamination during the cycling. All experiments were done at 1,600 rpm with a 20 mV $s^{-1}$ sweeping rate.

---

**References:**


(1) Shinagawa, T.; Garcia-Esparza, A. T.; Takanabe, K. *Sci. Rep.* **2015**, *5*, 13801.

(2) Strmcnik, D.; Uchimura, M.; Wang, C.; Subbaraman, R.; Danilovic, N.; van der Vliet, D.; Paulikas, A. P.; Stamenkovic, V. R.; Markovic, N. M. *Nat. Chem.* **2013**, *5*, 300–306.

(3) Eda, G.; Yamaguchi, H.; Voiry, D.; Fujita, T.; Chen, M.; Chhowalla, M. *Nano Lett.* **2011**, *11*, 5111–5116.

(4) Kappera, R.; Voiry, D.; Yalcin, S. E.; Branch, B.; Gupta, G.; Mohite, A. D.; Chhowalla, M. *Nat. Mater.* **2014**, *13*, 1128–1134.

(5) Calandra, M. *Phys. Rev. B* **2013**, *88* (24), 245428.